Global Phospholipidomics Analysis Reveals Selective Pulmonary Peroxidation Profiles upon Inhalation of Single-Walled Carbon Nanotubes

Yulia Y. Tyurina,[†,‡,*] Elena R. Kisin,[§] Ashley Murray,[§] Vladimir A. Tyurin,[†,‡] Valentina I. Kapralova,[†,‡] Louis J. Sparvero,[†,‡,⊥] Andrew A. Amoscato,[†,‡] Alejandro K. Samhan-Arias,[†,‡] Linda Swedin,[∥] Riitta Lahesmaa,[⊥] Bengt Fadeel,[∥] Anna A. Shvedova,[§] and Valerian E. Kagan[†,‡,*]

[†]Center for Free Radical and Antioxidant Health, [‡]Department of Environmental and Occupational Health, University of Pittsburgh, Pittsburgh, Pennsylvania, United States, [§]Pathology and Physiology Research Branch, Health Effects Laboratory Division, National Institute for Occupational Safety and Health (NIOSH), Morgantown, West Virginia, United States, [⊥]Turku Centre for Biotechnology, University of Turku and Åbo Akademi University, Finland, and [∥]Division of Molecular Toxicology, Institute of Environmental Medicine, Karolinska Institutet, Stockholm, Sweden

ABSTRACT It is commonly believed that nanomaterials cause nonspecific oxidative damage. Our mass spectrometry-based oxidative lipidomics analysis of all major phospholipid classes revealed highly selective patterns of pulmonary peroxidation after inhalation exposure of mice to single-walled carbon nanotubes. No oxidized molecular species were found in the two most abundant phospholipid classes: phosphatidylcholine and phosphatidylethanolamine. Peroxidation products were identified in three relatively minor classes of anionic phospholipids, cardiolipin, phosphatidylserine, and phosphatidylinositol, whereby oxygenation of polyunsaturated fatty acid residues also showed unusual substrate specificity. This nonrandom peroxidation coincided with the accumulation of apoptotic cells in the lung. A similar selective phospholipid peroxidation profile was detected upon incubation of a mixture of total lung lipids with H_2O_2/cytochrome *c* known to catalyze cardiolipin and phosphatidylserine peroxidation in apoptotic cells. The characterized specific phospholipid peroxidation signaling pathways indicate new approaches to the development of mitochondria-targeted regulators of cardiolipin peroxidation to protect against deleterious effects of pro-apoptotic effects of single-walled carbon nanotubes in the lung.

KEYWORDS: single-walled carbon nanotubes · mouse lung · apoptosis · lipidomics · oxidative lipidomics · cardiolipin oxidation · phosphatidylserine oxidation

Remarkable progress in nanotechnology has paved the way for a very broad utilization of different engineered nanomaterials, including single-walled carbon nanotubes (SWCNTs), for various technological and biomedical applications.[1−3] In spite of such impressive benefits, the unique physicochemical properties of SWCNTs have raised concerns about potential risks for human health associated with their use.[4] In fact, animal studies[5−7] as well as new epidemiologic data indicate that exposure to SWCNTs without sufficient protective measures may cause pulmonary toxicity, granuloma formation, chronic pulmonary inflammation leading to fibrosis, and also mutagenic effects in the lungs.[8,9] The generation of reactive oxygen species (ROS) culminating in severe oxidative stress is commonly viewed as a mechanism of nanomaterial-induced toxicity.[10,11] Indeed, ROS-driven peroxidation of lipids—particularly polyunsaturated phospholipids in cellular membranes—is considered to be one of the major mechanisms of lung injury triggered by SWCNTs.[12,13] In support of this notion, previous studies have shown that mice that are maintained on a diet deficient for vitamin E, the major lipid-soluble antioxidant, display an increased sensitivity to SWCNT-induced pulmonary inflammation and enhanced pro-fibrotic responses.[14]

In addition to the nonspecific deleterious effects of lipid peroxidation, oxidized phospholipids have also been recognized as important regulators of cell signaling, with essential physiological functions in signal transduction.[15−17] In particular, lipid peroxidation has been implicated in the execution of apoptosis (programmed cell death) and in the subsequent removal of apoptotic cell corpses by phagocytic cells of the immune system (programmed cell clearance), a process that is crucial for the resolution of inflammatory responses.[18−20] Moreover, enzymatic oxidation is involved in the biodegradation of SWCNTs by the neutrophil myeloperoxidase.[21] Therefore, peroxidation reactions may be viewed not only as a byproduct of cellular oxidative stress but also as an important signaling event in physiological as well as pathophysiological

* Address correspondence to kagan@pitt.edu or yyt1@pitt.edu.

Received for review June 15, 2011 and accepted July 30, 2011.

Published online July 31, 2011
10.1021/nn202201j

processes including responses to nanomaterial exposure.[22] Until recently, detailed analysis of pulmonary phospholipid peroxidation was not feasible. We have pioneered the field of oxidative lipidomics and developed quantitative approaches to identification and characterization of individual molecular species of peroxidized phospholipids in different tissues, including the lung, after exposure to a variety of insults.[21,23−25] Here, we performed global mass spectrometry (MS)-based oxidative lipidomics analysis of all major classes of pulmonary phospholipids to determine whether random or selective profiles are characteristic of the lung responses after the inhalation exposure of mice to SWCNTs.

RESULTS

SWCNT-Induced Inflammatory Pulmonary Response. We applied oxidative lipidomics protocols to reveal whether pulmonary responses to SWCNTs engage nonspecific phospholipid peroxidation processes or selective pathways involved in phospholipid-mediated signaling. In this study, we purposely utilized nonpurified commercial SWCNTs with high content of transition metals, particularly iron (up to 17.7 wt %), known to effectively catalyze nonspecific free radical peroxidation of polyunsaturated phospholipids. Toxicological assessment of such materials is relevant to human exposure to SWCNTs in the occupational setting. C57BL/6 mice were exposed to nonpurified SWCNT *via* inhalation (5 mg/m^3, whole body inhalation for 4 consecutive days, 5 h/day) and sacrificed 1, 7, and 28 days thereafter. In line with previous reports,[22,26] SWCNTs caused a robust inflammatory pulmonary response with a characteristic time-dependent recruitment of neutrophils and macrophages (Figure 1a) and the formation of persistent granulomas (Figure 1b). Notably, significantly elevated levels of apoptotic cells were observed on days 1 and 7, as evidenced by TUNEL staining (Figure 1c). An increased infiltration of myeloperoxidase-positive neutrophils was detected on day 1 and day 7 postexposure to SWCNTs when compared to air-exposed control mice. The increase of the number of neutrophils was more pronounced on 1 day of exposure (Figure 1d), which is in accordance with the quantification of the number of neutrophils recovered in bronchoalveolar lavage (BAL) (Figure 1a). In addition, an increased infiltration of macrophages—more pronounced on day 7 postexposure (data not shown)—was also observed in SWCNT-exposed mice compared to controls.

Lipidomics Analysis of Mouse Lung Phospholipids. To characterize possible SWCNT-induced changes in phospholipids, we performed lipidomics/oxidative lipidomics characterization of all molecular species in seven major classes of phospholipids in total lung tissue from exposed animals. The initial 2D high-performance thin-layer chromatography (2D-HPTLC) analysis of phospholipid classes did not reveal any significant changes in *total* phospholipid composition (without detailed MS analysis of individual molecular species) after SWCNT exposure (Figure 2).

The rate of nonenzymatic free radical lipid peroxidation very strongly depends on the level of lipid unsaturation, whereby the process propagates most effectively in phospholipids containing fatty acyls with six, five, and four double bonds, followed by phospholipids with three and two double bonds.[27] Monounsaturated and saturated phospholipids are highly resistant to peroxidation. The polar "head" of phospholipids is much less essential as a factor affecting the rate of stochastic free radical lipid peroxidation. In contrast, enzymatically catalyzed phospholipid peroxidation is very sensitive to the structure of the polar parts of phospholipid molecules recognized by specific protein catalysts.[28] By using MS analysis, we identified 135 individual molecular species of total phospholipids in the lung of control and SWCNT-exposed animals. Of those, 89 individual species were represented by polyunsaturated phospholipids, while 46 species of phospholipids were monounsaturated or saturated. This analysis conducted for seven major classes of phospholipids revealed that with the exception of sphingomyeline (Sph) and phosphatidylglycerol (PG), which contained predominantly saturated and monounsaturated species, all other phospholipids included a variety of highly oxidizable polyunsaturated species (Figure 3). The ranking order of nonenzymatic free radical "oxidizability" of phospholipids defined as the product of the content of polyunsaturated molecular species times phospholipid abundance decreased in the order phosphatidylcholine (PC) > phosphatidylethanolamine (PE) > phosphatidylinositol (PI) > phosphatidylserine (PS) > cardiolipin (CL). Thus, PC and PE represented the most likely candidates as substrates for random free radical peroxidation in the lung.

Oxidative Lipidomics of SWCNT-Induced Lung Injury. Next, we performed oxidative lipidomics analysis of the lung phospholipids in exposed *vs* control mice. Surprisingly, we did not detect any oxidized molecular species in the two most abundant (constituting more than 75% of all) phospholipids—PC and PE—which should have been highly susceptible to nonenzymatic free radical peroxidation. Instead, three relatively minor anionic phospholipids—CL, PS, and PI—underwent peroxidation (Table S1). The magnitude of the effect was particularly pronounced in CL. To directly characterize the peroxidized CL species, the CL "spots" obtained by HPTLC separation were analyzed by 2D-liquid chromatography (LC)/MS, whereby a reverse-phase chromatography was utilized in the second dimension. We were able to resolve nonoxidized from peroxidized species of CL that differed significantly in their retention times. In the control samples, we detected the abundant nonoxidized CL species with only small amounts of three types of peroxidized CLs corresponding to monohydroperoxy or/and dihydroxy molecular

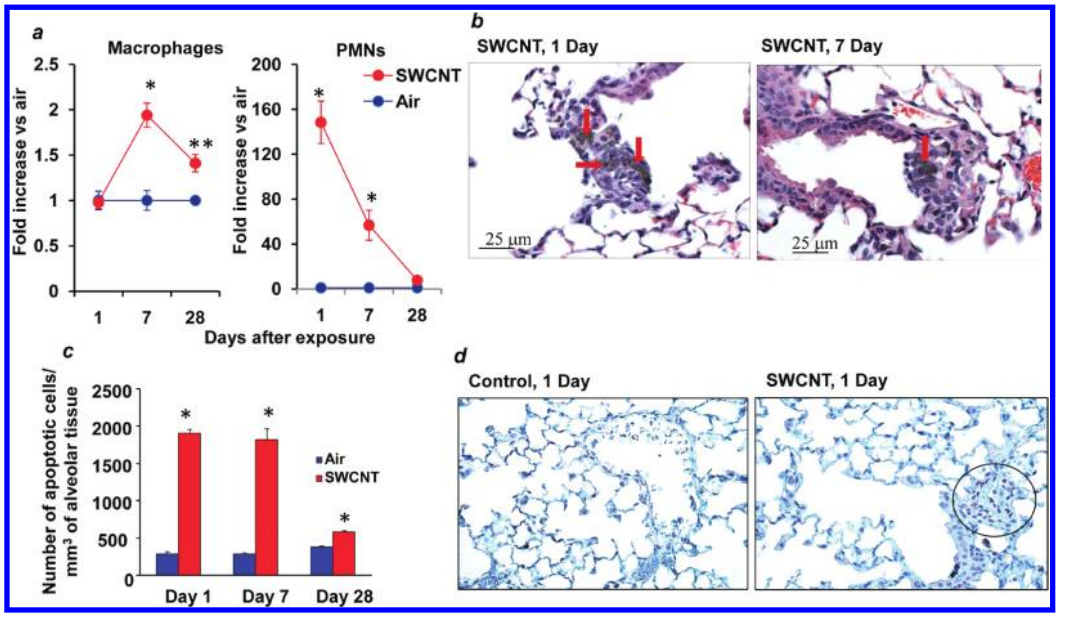

Figure 1. SWCNT-induced pulmonary inflammatory response. (a) Cell profile in bronchoalveolar lavage (BAL) fluids of C57BL/6 mice after inhalation of SWCNTs (5 mg/m^3, 5 h/day, 4 days). Left panel: alveolar macrophages. Data are means ± SD, $n = 7$; *$p < 0.001$ *vs* control mice (exposed to air); **$p < 0.004$ *vs* control mice (exposed to air). Right panel: polymorphonuclear leukocytes (PMNs). Data are means ± SD, $n = 7$; *$p < 0.001$ *vs* control mice (exposed to air); *$p < 0.001$ *vs* control mice (exposed to air). (b) Histopathology of lung sections from mice exposed to SWCNTs (5 mg/m^3, 5 h/day, 4 days). Left panel: 1 day after last SWCNT exposure; aggregates of SWCNTS are seen frequently free near bronchiole−alveolar junctions. Right panel: 7 days after the last SWCNT exposure; there are multinucleated cells with dark brown foreign (SWCNT) materials, granulomatous lesions, and fibrosis. Typical micrographs are presented. Arrows indicate aggregates of SWCNT. (c) Total apoptosis-positive cells per mm^3 of alveolar tissue of the lung from C57BL/6 mice in response to inhalation of SWCNTs (5 mg/m^3, 5 h/day, 4 days). Data are means ± SD; $n = 7$; *$p < 0.001$ *vs* control mice (exposed to air). (d) Myeloperoxidase staining. Left panel: Air-exposed controls. Right panel: 1 day after last SWCNT exposure. Increased numbers of neutrophils (circled) could be observed in SWCNT-exposed mice. Typical micrographs are presented.

species of CL. These oxidized CL species were also observed in the lungs from SWCNT-exposed mice (day 7) at approximately a 3-fold higher intensity. An additional monohydroxy-monohydroperoxy-CL species was present in the 7-day SWCNT sample. These oxidized species could be generated from nonoxidized CL species $C_{18:1}/C_{18:2}/C_{18:2}/C_{16:0}$, $C_{18:2}/C_{18:2}/C_{18:2}/C_{20:4}$, $C_{18:2}/C_{18:2}/C_{18:1}/C_{20:4}$, and $C_{18:2}/C_{18:1}/C_{18:1}/C_{20:4}$ upon addition of three, two, two, and two oxygens, respectively, thus representing combinations of hydroxy- and/or hydroperoxy-modifying groups (Figure 4). Profiles for the nonoxidized CL species for the control and the SWCNT-exposed groups were essentially identical (Figure 4). In line with these 2D-LC/MS data, ESI-MS analysis revealed a significant decrease of polyunsaturated molecular species of CL—caused by their involvement in the peroxidation reactions—in the lung of mice exposed to SWCNTs (Figures S1 and S2). Oxidation of CL on day 7 postexposure was further confirmed by another type of MS analysis, MALDI-TOF-MS (Figure S3), which allows for the analysis of predominantly singly charged species and the ability to reanalyze the sample, thus alleviating the disadvantage of analyzing the oxidized species during a specified timed event (*i.e.*, the elution of the chromatographic peak) during traditional LC/MS analysis. Significantly decreased levels of "oxidizable" species were documented by MS analysis of two other classes of pulmonary anionic phospholipids—PS and PI—obtained from SWCNT-exposed mice.

Identification of Oxygenated Fatty Acids. To more completely characterize the nature of oxygenated species in anionic phospholipids, we further performed MS/MS analysis of these phospholipids as well as their hydrolysis products formed after treatment with phospholipase A_2 (PLA_2) (Figures S4 and S5). These measurements revealed yet another level of specificity of the peroxidaion process: within each class of anionic phospholipids, the peroxidation pattern displayed a nonrandom character; only a few molecular species out of many (10 out of 23 for CL, 1 out of 7 for PS, and 3 out of 5 for PI) were converted into oxygenated species (Figure 5).

The specificity was also detected toward fatty acids of the oxidized anionic phospholipids (Figure 6). Surprisingly, among the polyunsaturated CLs and PSs, the species containing fatty acid residues with two double bonds—$C_{18:2}$—underwent oxidative modification to mono- (13-OH-$C_{18:2}$ and 9-OH-$C_{18:2}$) and dihydroxy (13-,8-diOH-$C_{18:2}$ and 9-,14-diOH-$C_{18:2}$) as well as monohydroperoxy (13-OOH-$C_{18:2}$ and 9-OOH-$C_{18:2}$) molecular species, whereas more polyunsaturated fatty acid residues such as $C_{20:4}$, and $C_{22:6}$—known to be more readily "oxidizable" in nonenzymatic free radical reactions—remained nonoxidized. Small

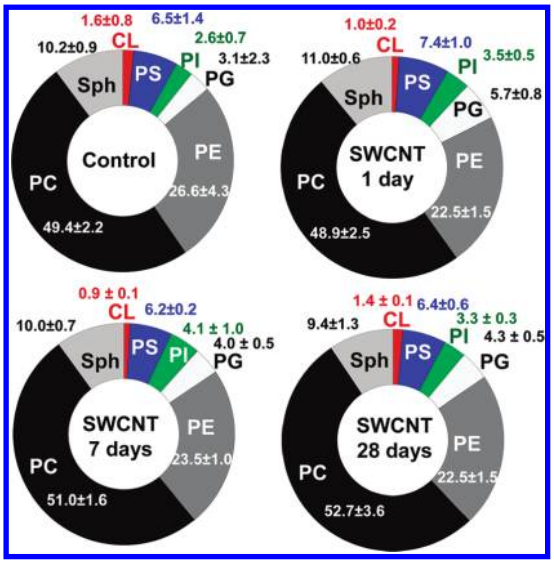

Figure 2. Phospholipid composition of the lung from control and SWCNT-treated mice on days 1, 7, and 28 after exposure. Lipids from lungs of control mice and mice exposed to SWCNTs were isolated and resolved by 2D-HPTLC. Spots of phospholipids were visualized by iodine vapors. After that, spots were scraped and lipid phosphorus was detected. The content of phospholipids was expressed as percent of total phospholipids. Data are means ± S.D, n = 3−5. After exposure to SWCNTs, no detectable differences in phospholipid content or in phospholipid composition of the lungs were found. CL = cardiolipin; PS = phosphatidylserine; PI = phosphatidylinositol; PG = phosphatidylglycerol; PE = phosphatidylethanolamine; PC = phosphatidylcholine; Sph = sphingomyelin.

amounts of PI oxidative molecular species containing OH-$C_{20:4}$ were detected (Figure 6).

Cyt *c*-Driven Phospholipid Oxidation. To gain insight into possible mechanisms involved in SWCNT-triggered phospholipid oxidation in mouse lung, we performed *in vitro* model experiments. Because we documented both increased amounts of apoptotic cells as well as CL and PS oxidation on days 1 and 7 after SWCNT exposure, we reasoned that the substrate specificity of the peroxidation process might be related to the execution of the apoptotic program. Our previous work has identified cyt *c*/H_2O_2 as the catalyst of CL and PS peroxidation in apoptotic cells *in vitro* and *in vivo*.[6,29−33] Therefore, we performed LC-MS measurements in total lipids extracted from mouse lung oxidized by cyt *c*/H_2O_2. Intriguingly, lipidomics analysis revealed a pattern of selective oxidation of anionic phospholipids—CL, PS, and PI—similar to that detected in the lung of mice exposed to SWCNTs (Figure 5). No oxidation of either PE or PC was detected. This is compatible with an interpretation that apoptotic cyt *c*-driven oxidation reactions are involved, at least in part, in the selective peroxidation of phospholipids after SWCNT inhalation.

DISCUSSION

In this inhalation study, we chose to perform our assessments using a cumulative dose of 5 mg/m^3, 5 h, 4 days. The dose−responses of SWCNT exposure causing pulmonary damage/toxicity in C56BL6 mice were addressed in our previous publications.[6,26] Pharyngeal aspiration exposure of mice to respirable SWCNTs within the 5, 10, and 20 μg SWCNT/mouse range was found to efficiently induce dose-dependent pulmonary damage, interstitial fibrosis, and granulomatous lesions in mouse lungs. Even though there has been a concern that pharyngeal aspiration as a single exposure to a bolus of SWCNTs may induce artificial response, it has been shown to closely mimic the inhalation exposure route and is currently accepted for assessments of health outcomes of respirable particles and infectious agents. Comparison of the pulmonary/toxicological data obtained from inhalation *vs* pharyngeal aspiration studies revealed that the calculated deposited dose of SWCNTs used in this inhalation study (5 mg/m^3, 5 h, 4 days) was 5 μg/mouse. Therefore, the exposure level in the current inhalation study was designed on the basis of adverse outcomes found from an equivalent mass of deposited SWCNTs used in pharyngeal aspiration protocols. Additionally, the rationale for use of 5 mg/m^3 dose for the inhalation study is based on the permissible exposure level (PEL) set by OSHA for respirable synthetic graphite dust that is currently applied to SWCNTs. This dose would be achieved by workers exposed for less than 2 years at the peak airborne concentrations measured in an occupational setting.[34] On the basis of the data obtained from the inhalation study, it could be inferred that if workers were subjected to extended exposures to respirable SWCNTs at current PEL for synthetic graphite, they would likely have an increased risk of pulmonary damage. The dose of SWCNTs used in this inhalation study may also be compared with regulatory permissible levels established for ambient microparticles, similar to those that the EPA established for $PM_{2.5}$, 65 μg/m^3 (24 h daily) and 15 μg/m^3 (annual average).[35]

Some level of oral exposure and systemic distribution of SWCNT can take place during the prolonged SWCNT inhalations. In our experiments, mice were cleaned following daily inhalation exposures and then placed into new cages to minimize/avoid the potential for oral consumption of SWCNTs during the night. The data regarding the oral toxicity of SWCNT in mice are scarce. Deng *et al.*[36] demonstrated that, after oral administration of multiwalled carbon nanotubes (MWCNTs) (10 μg/mouse), the majority of nanoparticles remained within the stomach and small and large intestines, with no detectable transport into the bloodstream. MWCNTs found in the gut remained unchanged. Similarly, no SWCNT translocation was reported by Folkmann *et al.*[37] After oral administration to rats, no detectable levels of SWCNTs were found in the lung and liver.

Our results demonstrate that phospholipid peroxidation in the lungs of mice exposed to SWCNT *via*

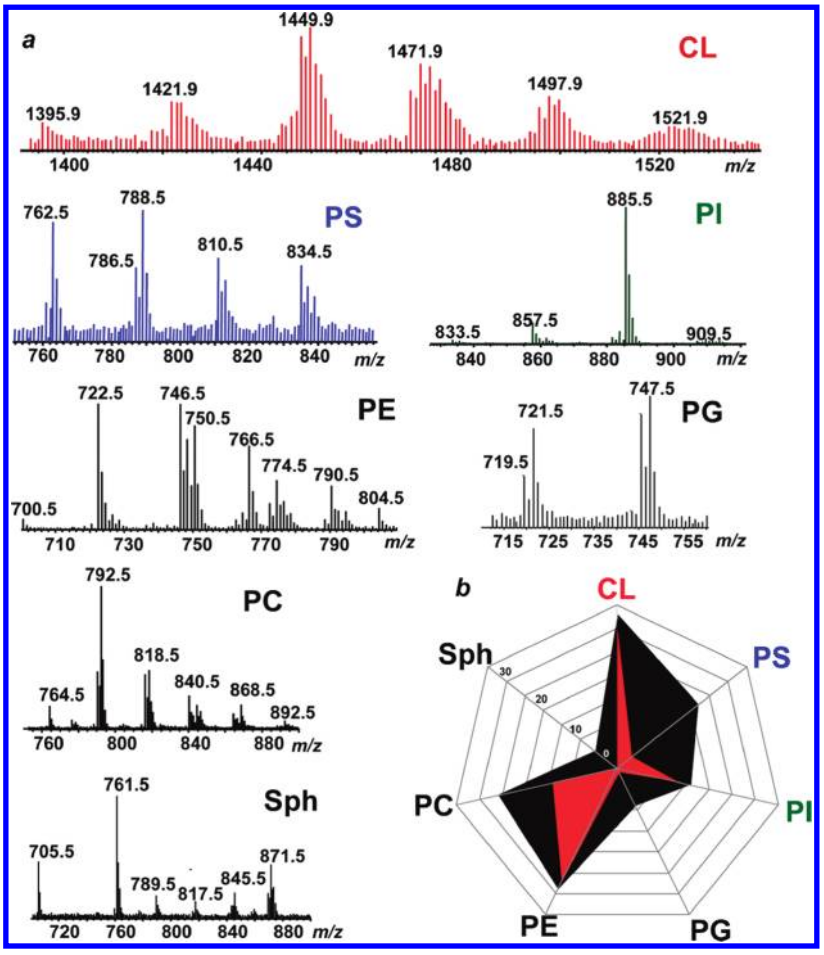

Figure 3. Assessment of different phospholipid classes in mouse lung using the lipidomics approach. (a) Typical full negative LC/ESI-MS spectra of phospholipids isolated from control mouse lung. Molecular species of phospholipids were characterized by LC/ESI-MS using the negative mode. The five molecular clusters containing molecular ions with *m/z* 1447.9, 1421.9, 1473.9, 1497.9, and 1521.9 were detectable in the full MS spectrum of CL. Molecular species of lung CL were identified and characterized by ESI-MS.[43] Mouse lung CL was enriched with molecular species containing linoleic acid ($C_{18:2}$) (*m/z* 1447.9, $C_{18:2}/C_{18:2}/C_{18:2}/C_{18:2}$; 1449.9, $C_{18:2}/C_{18:2}/C_{18:2}/C_{18:1}$; *m/z* 1451.9, $C_{18:2}/C_{18:2}/C_{18:1}/C_{18:1}$; 1453.9, $C_{18:2}/C_{18:1}/C_{18:1}/C_{18:1}$). CL molecular species, containing at least one polyunsaturated acyl group with four, five, and six double bonds were also detected (*m/z* 1467.9, $C_{18:2}/C_{18:2}/C_{18:2}/C_{20:4}$; *m/z* 1469.9, $C_{18:2}/C_{18:2}/C_{18:3}/C_{20:4}$; 1471.9, $C_{18:2}/C_{18:2}/C_{18:2}/C_{20:4}$; 1473.9, $C_{18:1}/C_{18:2}/C_{18:2}/C_{20:4}$; 1475.9, $C_{18:1}/C_{18:1}/C_{18:2}/C_{20:4}$; *m/z* 1493.9, 1495.9, $C_{18:2}/C_{18:2}/C_{20:4}/C_{20:4}$; 1497.9, $C_{18:1}/C_{18:2}/C_{20:4}/C_{20:4}$; $C_{18:1}/C_{18:2}/C_{18:2}/C_{22:6}$; 1499.9, $C_{18:1}/C_{20:4}/C_{20:4}/C_{18:1}$; $C_{18:0}/C_{18:2}/C_{18:2}/C_{22:6}$; $C_{18:0}/C_{18:2}/C_{18:2}/C_{22:6}$; $C_{18:1}/C_{18:2}/C_{18:2}/C_{22:5}$). The molecular ions of PS with *m/z* 786.5, 788.5, 810.5, 812.5. 834.5, 836.5, and 836.5 corresponded to $C_{18:0}/C_{18:2}$, $C_{18:0}/C_{18:1}$, $C_{18:0}/C_{20:4}$, $C_{18:0}/C_{20:3}$, $C_{18:0}/C_{22:6}$, $C_{18:0}/C_{22:5}$, and $C_{18:0}/C_{22:4}$ molecular species, respectively. Molecular species of lung PI were represented by predominant molecular species with *m/z* 885.5 corresponding to $C_{18:0}/C_{20:4}$ and less abundant species with *m/z* 857.5 and 833.5 corresponding to $C_{16:0}/C_{20:4}$ and $C_{16:0}/C_{18:2}$, respectively. PG with *m/z* 721.5, 745.5, and 747.5 containing mostly saturated fatty acids was identified as $C_{16:0}/C_{16:0}$, $C_{16:0}/C_{18:2}$, and $C_{16:0}/C_{18:1}$. (b) Susceptibility of mouse lung phospholipids to oxidation. Black = total number of molecular species of major lung phopsholipids. Red = number of oxidizable molecular species of lung phospholipids. CL = cardiolipin, PS = phosphatidylserine, PI = phosphatidylinositol, PG = phosphatidylglycerol, PE = phosphatidylethanolamine, PC = phosphatidylcholine, Sph = sphingomyelin.

inhalation does not exert the features typical of a random free radical process but instead displays high substrate and product specificity, thus suggesting the involvement of enzymatic mechanisms. There are at least two important consequences from this finding: First, because nonspecific radical scavenging antioxidants are not expected to be effective in suppressing enzymatically driven lipid peroxidation, their application as protectants against SWCNT-induced pulmonary damage is questionable. Second, the current observations suggest that exposure to SWCNTs triggers specific pathways of cellular damage, which implies that the adverse effects elicited by SWCNTs could be counteracted by targeting these pathways, likely apoptotic in nature.

Mitochondrial signaling is central to the execution of several death pathways, including apoptosis. Upon activation of mitochondria by various pro-apoptotic stimuli, cyt *c*, a small hemoprotein of the intermembrane space of these organelles, is released into the cytosol and acts as a cofactor for the apoptosome complex, a multicomponent platform that promotes the activation of caspases, with subsequent cleavage of target proteins and dismantling of the cell.[38] We

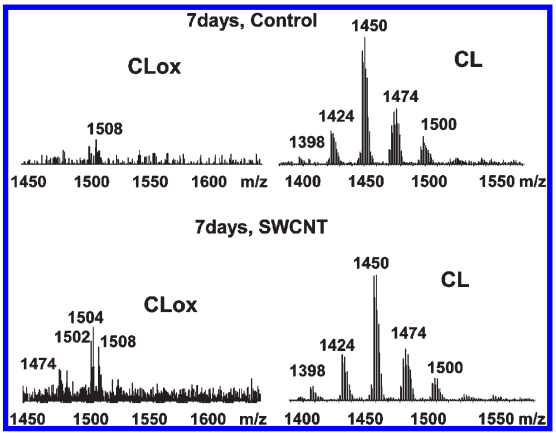

Figure 4. 2D-LC/MS profiles and MS spectra of CL from control lung and lung of mice on day 7 post (SWCNT)-inhalation. CL fractions were analyzed by LC-MS using a C_8 column and an isocratic solvent system (2-propanol/water/triethylamine/acetic acid (450:50:2.5:2.5, v/v/v/v). Oxidized and nonoxidized CL species typically elute in a 4−6 min and 6−8 min retention time window, respectively. Oxidized CL species were detected in both the 7-day control sample (top panel) and the 7-day SWCNT sample (bottom panel). CL oxidized species with *m/z* 1474, 1502, 1504, and 1508 in the SWCNT sample were present in higher abundance. A smaller number and lower magnitude of the signals corresponding to oxidized species (*m/z* 1502, 1504, and 1508) were detected in MS spectra from the lung lipids of control mice.

have previously ascertained that cyt *c* can effectively catalyze peroxidation of anionic phospholipids, particularly CL, but also PS and PI.[28] Moreover, this cyt *c*-catalyzed pathway was found to play an important role in the execution of apoptosis.[6] It has been shown that CL and its oxidation products are important participants and signaling molecules in the mitochondria-dependent apoptotic cell death program.[39] Early in apoptosis, massive membrane translocations of CL result in the appearance of CL in the outer mitochondrial membrane.[39] Consequently, significant amounts of CL become available for the interactions with cyt *c*, one of the intermembrane space proteins. Binding of CL with cyt *c* yields a complex that acts as a potent CL-specific peroxidase[40] and generates CL peroxidation products that are important for the mitochondria permeabilization and the release of cyt *c* and other pro-apoptotic factors form mitochondria into the cytosol.[39] Given that the exposure to SWCNTs triggers the peroxidation of CL in the lungs of exposed animals, one may surmise that mitochondrial apoptotic signaling is engaged in pulmonary response to SWCNT exposure. In support of this contention, the numbers of apoptotic cells in the lungs of exposed animals paralleled the selective peroxidation of lipids. Indeed, significant accumulation of apoptotic cells was observed on days 1 and 7 after SWCNT exposure, as determined by TUNEL staining.

The detection of increased numbers of apoptotic cells *in vivo* could in principle be explained by an excessive rate of apoptosis and/or a decreased capacity for macrophage clearance of apoptotic cell corpses. These observations are in line with the outcome of our oxidative lipidomics assessment that showed the selective peroxidation of PS and CL (and PI), while the more abundant phospholipids PC and PE were not affected upon pulmonary exposure to SWCNTs. Moreover, this interpretation is supported by our model experiments with the mouse lung phospholipids incubated with cyt *c* and H_2O_2. These experiments demonstrate a very similar pattern of selectivity with predominant peroxidation of the same molecular species of CL, PS, and PI as in mice exposed to SWCNTs. In other words, it is possible that mitochondrial apoptosis with cyt *c*-driven peroxidation of CL and PS could explain the observed pattern of lipid peroxidation in the lungs of mice exposed to SWCNTs. However, we cannot exclude the involvement of NADPH oxidase-derived ROS, particularly at later stages of the inflammatory response. In a previous study, we showed that NADPH oxidase-deficient mice displayed increased and persistent accumulation of neutrophils and elevated levels of apoptotic cells in the lungs and significantly decreased fibrotic responses to SWCNT when compared to wild-type mice.[7] This suggests a role for NADPH oxidase-derived ROS in determining the course of pulmonary response to SWCNTs.

Our previous work has identified the enzymatic process of CL peroxidation as a potentially important target for the discovery of mitochondria-targeted antiapoptotic small molecule protectors.[41,42] Two different types of these molecules have been designed: GS-nitroxides, conjugates of stable nitroxide radicals with mitochondria-targeting hemigramicidin S, and TPP-IFFAs, conjugates of imidazole-substituted fatty acids (oleic and stearic) with mitochondria-targeting triphenyl-phosphonium. GS-nitroxides act as electron-scavengers effective in preventing the production of superoxide radicals and its dismutation product, H_2O_2, in mitochondria. Because H_2O_2 feeds the peroxidase cycle involved in the catalysis of CL peroxidation, GS-nitroxides turned out to be effective in inhibiting CL peroxidation.[41−43] TPP-IFFAs act through a different mechanism: they are strong ligands of heme-iron in cyt *c*/CL complexes that block their peroxidase activity toward peroxidation of CL. Both of these newly designed small molecule regulators displayed pronounced antiapoptotic properties *in vitro* and *in vivo*, for example as protectors/mitigators against apoptotic damage[44] and acute radiation syndrome induced by total body irradiation.[45] Assuming that apoptosis is an essential contributor to the SWCNT-induced lung injury, we suggest that our discovered specificity of CL peroxidation indicates a possibility of using the mitochondria-targeted GS-nitroxides and TPP-IFFAs as potentially useful regulators of CL peroxidation and antiapoptotic protectors in the lung.

Following the induction of cell death by apoptosis, cell corpses are removed by professional phagocytes

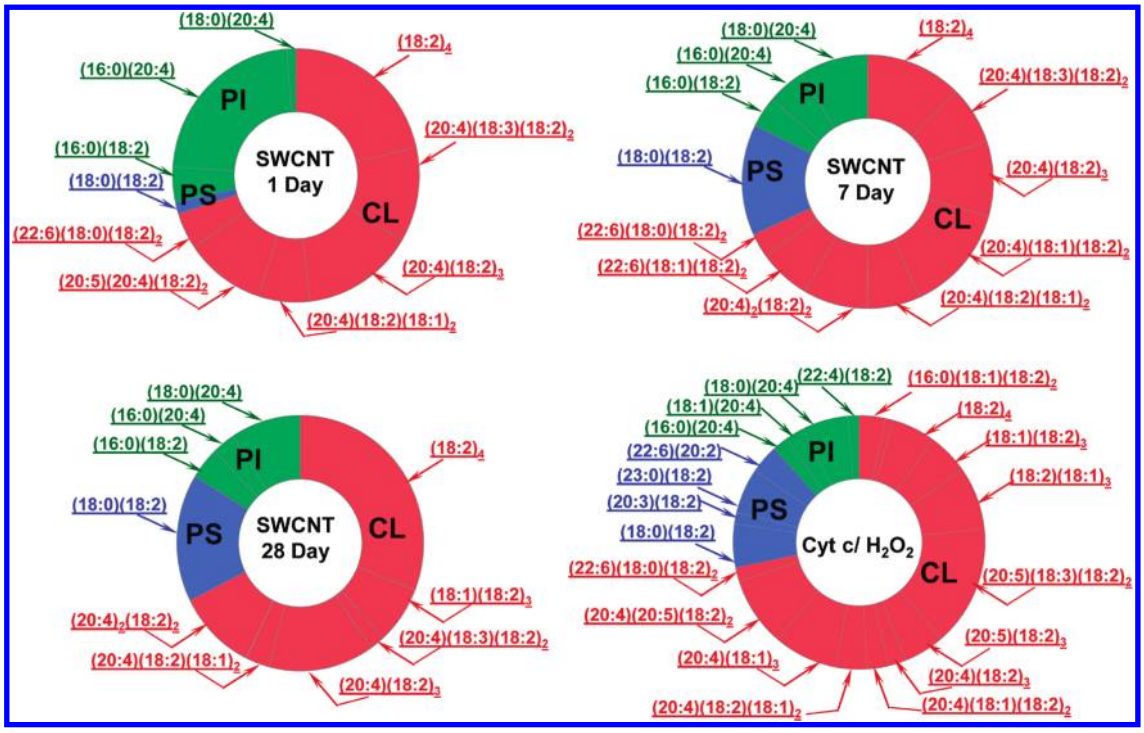

Figure 5. Profiles of phospholipid oxidation in the lung induced by the exposure of mice to SWCNTs and by incubation of phospholipids extracted from the lung in a model system containing cyt *c* and H_2O_2. Lipids from lungs of control mice and mice exposed to SWCNTs were isolated and resolved by LC/MS. The data are presented as decreases in the amounts of oxidizable molecular species of phospholipids after exposure to SWCNTs. The total decreases of CL, PS, and PI amounts were 32.3, 0.7, and 13.1 pmol/nmol of phospholipid, respectively, on day 1 postexposure. On days 7 and 27 after the exposure, the decreases of CL, PS, and PI contents were 62.2, 12.9, 16.1 and 32.7, 7.8, 7.9 pmol/nmol of phospholipid, respectively. Model system: lung lipids (500 μM) were sonicated and incubated with cyt *c* (10 μM) in the presence of H_2O_2 (100 μM) for 30 min at 37 °C. At the end of the incubation, lipids were extracted and CL molecular species were quantitatively assessed by LC/MS. The data are presented as decreases in the amounts of oxidizable molecular species of phospholipids after incubation with cyt *c* in the presence of H_2O_2. The decreases of CL, PS, and PI were 80.8, 18.5, and 9.5 pmol/nmol of phopsholipid. Oxidation of lung phospholipids in this model system resulted in predominant peroxidation of the same molecular species of CL, PS, and PI as in mice exposed to SWCNTs. CL = cardiolipin, PS = phosphatidylserine, PI = phosphatidylinositol.

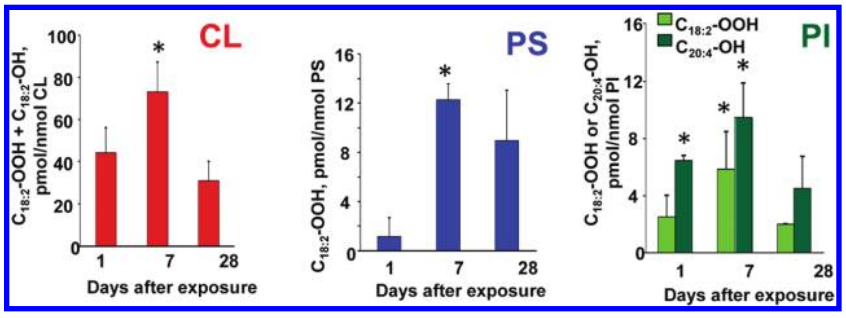

Figure 6. Quantitative assessments of oxygenated fatty acid residues in CL, PS, and PI isolated from the lung of mice exposed to SWCNTs. The data are presented as increases in the amounts of oxygenated fatty acids released from the phospholipids after treatment with PLA_2. PLA_2 hydrolysis of CL, PS, and PI and subsequent MS analysis of fatty acid profiles confirmed the presence in the lung of OOH-$C_{18:2}$, OH-$C_{18:2}$, and OH-$C_{20:4}$. Data are means ± SD, $n = 3-5$, $^*p < 0.05$ *vs* control. The values for OOH-$C_{18:2}$ and OH-$C_{18:2}$ hydrolyzed from CL in control samples were in the range 59.4−68.8 pmol/nmol of total fatty acids released by PLA_2 from CL. The values for $C_{18:2}$-OOH hydrolyzed from PS in control samples were in the range 14.3−15.1 pmol/nmol of total fatty acids released by PLA_2 from PS. The values for OOH-$C_{18:2}$ and OH-$C_{20:4}$ hydrolyzed from PI in control samples were 20.0−24.5 and 2.0−9.0 pmol/nmol of total fatty acids released by PLA_2 from PI, respectively. CL = cardiolipin, PS = phosphatidylserine, PI = phosphatidylinositol.

or neighboring cells in order to avoid tissue damage, which would otherwise occur due to the persistent exposure to cell debris and the ensuing leakage of noxious intracellular constituents. In particular, macrophage clearance of apoptotic neutrophils at sites of inflammation is believed to be required for the effective resolution of the inflammatory process.[46] Released cyt *c* forms cyt *c*/PS complexes that act as major catalysts of PS oxidation and subsequent PS externalization during late stages of apoptosis.[47,48]

Externalized PS and its peroxidation products are essential "eat-me" signals for macrophage engulfment and clearance of apoptotic cells (reviewed in ref 49). We and others have shown that the externalization of oxidized PS on the surface of apoptotic cells is required for their effective clearance by macrophages.[50−52] Moreover, the absence of PS oxidation and exposure in neutrophils derived from patients with chronic granulomatous disease leads to the ineffective clearance by macrophages, suggesting a critical role for PS exposure and oxidation in the prevention of chronic inflammation in humans.[53] The current observation of specific peroxidation of PS in the lungs of exposed mice suggests that the pathways of PS-dependent clearance of apoptotic cells may be important in tissue responses to SWCNT. It is also tempting to speculate that oxygenated species of CL, PS, and PI are essential precursors of inflammatory regulators such as resolvins.[15,16] Indeed, small amounts of oxygenated docosahexaenoic acid-containing species of PS—potential substrates of PLA_2 attack[54]—have been detected after SWCNT exposure.

Using similar oxidative lipidomics protocols, we have previously characterized the pattern of phospholipid peroxidation following several other insults, including hyperoxic acute lung injury, γ-radiation-induced lung injury, and traumatic brain injury.[21,24,29] Strikingly, in all cases, a selective pattern of phospholipid peroxidation involving primarily CL and/or PS was observed. The fact that inhalation exposure to SWCNTs with high content of transition metals, particularly iron, known to effectively catalyze nonspecific peroxidation of polyunsaturated phospholipids, also induces a similar, selective pattern of peroxidation of phospholipids suggests that common pathways of cellular and tissue damage are engaged, thus suggesting that SWCNTs do not elicit "nano-specific" effects. This is encouraging because it implies that common "antiapoptotic" countermeasures against a diverse range of insults, including nanomaterials, may be envisioned. The manufacturing of nanotube material relies on the use of transition metal catalysts. Most of the iron is present in elemental form, but its redox-active fraction in ionic form within carbonaceous particles may act as a catalyst of oxidative stress in biological settings. The major toxicity mechanisms induced by SWCNTs include inflammatory response and oxidative stress. Because inflammatory cells generate superoxide radicals and their dismutation product, H_2O_2, this provides a redox environment in which transition metals can fully realize their pro-oxidant potential, thus synergistically enhancing damage of iron-containing SWCNTs to cells and triggering cell death programs. Our previous work has characterized apoptosis-associated phopholipid peroxidation and revealed its selectivity in predominant peroxidation of two anionic phospholipids, CL and PS.[39,47] This selectivity was due to the central catalytic role of mitochondrial cyt *c* capable of forming peroxidase complexes with CL in mitochondria and with PS in extramitochondrial compartments of cells. SWCNT-associated iron may also *directly* induce lipid peroxidation reactions in cells and biofluids. As a random catalytic process, this reaction prefers the most abundant phospholipids with polyunsaturated fatty acid residues independently of their polar heads such as PC and PE. Notably, we found accumulation of peroxidized molecular species mostly in anionic phospholipids, CL and PS, while PC and PE remained essentially nonoxidized. This suggests that the apoptosis-associated phospholipid peroxidation process was dominant, while random catalytic reactions were a relatively minor contributor to the overall peroxidation. Interestingly, similar relationships were established in another type of pro-oxidant environment—total body irradiation, a well-known inducer of free radicals—whereby selective accumulation of peroxidation products in the lung was also detected only in CL and PS (but not in PC and PE).[24]

In conclusion, using global oxidative lipidomics, we characterized, for the first time, the specific peroxidation profiles of cellular phospholipids in the lungs of mice exposed to nonpurified (iron-containing) SWCNTs. This study thus indicates that the exposure to SWCNTs results in a selective lipid peroxidation rather than in nonspecific free radical oxidation.[55,56] Furthermore, the fact that we could detect specific peroxidation of CL and PS, and a concurrent elevation in the number of apoptotic cells, suggests the involvement of mitochondria-dependent apoptosis as well as macrophage disposal of apoptotic cells in the regulation of the inflammatory response to SWCNTs. Further studies are warranted to uncover the source(s) of selective, likely enzymatic, lipid peroxidation triggered by exposure to SWCNTs. In addition, oxidative lipidomics protocols may be applied to the study of other engineered nanomaterials, in the lung or in other tissues.

METHODS

Particles. SWCNTs were purchased from Carbon Nanotechnology (CNI, Houston, TX). The nanotubes were manufactured using the high-pressure CO disproportionation process (HiPco) and were used in the inhalation studies. The supplied SWCNTs contained nanometer-scale Fe catalyst particles inherent to the HiPco process. These SWCNTs contained elemental carbon (82 wt %) and Fe (17.7%). Trace elements present included Cu (0.16%), Cr (0.049%), and Ni (0.046%). Raman spectroscopy, near-infrared spectroscopy, and thermogravimetric analysis were used for purity assessment of HiPco SWCNTs. The spectra of the SWCNT sample revealed distinct peaks at a Raman shift of 1586−1591 cm^{-1}, corresponding to the characteristic G band of SWCNTs as well as D and G^1 bands typically found in SWCNT

spectra. The diameter of the SWCNT measured by transmission electron microscopy was 0.8−1.2 nm. The length of the SWCNT was 100−1000 nm as measured by atomic force microscopy. The surface area of the SWCNT measured by the nitrogen absorption−desorption technique (Brunauer−Emmett−Teller method) was 508 m^2/g.

Exposure of Mice to SWCNTs. C57BL/6 mice were exposed to SWCNTs *via* inhalation (5 mg/m^3, whole body inhalation for 4 consecutive days, 5 h/day).[26] All procedures were preapproved and performed according to the protocols established by the NIOSH Institutional Animal Care and Use Committee and the Institutional Animal Care and Use Committee of the University of Pittsburgh.

Obtaining Bronchoalveolar Lavage from Mice. Mice were sacrificed with intraperitoneal injection of sodium pentobarbital (>100 mg/kg) and exsanguinated. The trachea was cannulated with a blunted 22 gauge needle, and BAL was performed using cold sterile PBS at a volume of 0.9 mL for the first lavage (kept separate) and 1.0 mL for subsequent lavages. Approximately 5 mL of BAL fluid per mouse was collected in sterile centrifuge tubes. Pooled BAL cells for each individual mouse were washed in PBS by alternate centrifugation (800*g*, 10 min, 4 °C) and resuspension.

BAL Cell Counting and Differentials. The degree of inflammatory response was estimated by macrophages and polymorphonuclear leukocytes (PMNs) recovered by BAL. Total cell counts were performed using an electronic cell counter equipped with a cell sizing attachment (Coulter model Multisizer II with a 256C channelizer, Coulter Electronics, Hialeah, FL). Alveolar macrophages and PMNs were identified by their characteristic cell shape in cytospin preparations stained with Diffquick (Fisher Scientific, Pittsburgh, PA), and differential counts of BAL cells were carried out. Three hundred cells per slide were counted.

Lung Preparation for Microscopic Evaluation. Preservation of the lung was performed using protocols previously employed to study pulmonary effects of SWCNTs.[6] Briefly, animals were deeply anesthetized with an overdose of sodium pentobarbital, the trachea was cannulated, and clearing solution (saline with 100 U/mL heparin, 350 mosM sucrose) was perfused to clear blood from the lungs. The perfusate was then switched to the fixative. Coronal sections were cut from the lungs. The lungs were embedded in paraffin and sectioned at a thickness of 5 μm with an HM 320 rotary microtome (Carl Zeiss, Thornwood, NY). Lung sections for histopathologic evaluation were stained with hematoxylin and eosin and examined by a board certified veterinary pathologist for morphological alterations.

Detection of Apoptotic Cells in the Lung of Mice after SWCNT Inhalation. Cell apoptosis was determined by a fluorescence labeling apoptosis detection system (Promega, Madison, WI). This system measures fragmented DNA in apoptotic cells by catalytically incorporating fluorescein 12 dUTP at the 3′-OH ends using the TUNEL (TdT-mediated dUTP nick end labeling) assay. Normal cells were fluorescently labeled red by counterstaining with propidium iodide. Positive control slides were prepared by treating sections with DNase prior to TUNEL. Negative control slides were prepared by omission of the TdT enzyme from the labeling solution. The number of TdT positive nuclei enclosed by a cell cytoplasm (apoptotic cells) per unit area was counted in 10 randomly selected fields (40×) from each animal. Cell counts were expressed as the number of apoptotic cells per unit area of section.

Myeloperoxidase Staining. Lung sections were hydrated with tap water, and antigen retrieval was performed in citrate buffer solution, pH 6.0. The slides were pretreated with 3% hydrogen peroxide for 20 min to inhibit endogenous peroxidase and blocked using 2.5% normal horse serum (Vector Laboratories, Burlingame, CA) for 30 min to prevent nonspecific reactivity. Sections were incubated with anti-myeloperoxidase primary antibody (1:100, 4 °C overnight incubation) (ab9535, AbCam, Cambridge, UK). Then, sections were treated with a peroxidase conjugated secondary antibody (ImmPRESS, MP-7401, Vector Laboratories) for 30 min at RT. After washing, color was developed by adding AEC Chromogen for 10 min (SK-4200, Vector Laboratories). Finally, slides were counterstained with hematoxylin and mounted using Faramount (DAKO, Glostrup, Denmark). Negative control sections were treated in the same way, but primary antibodies were omitted. For the detection of macrophages, sections were incubated with anti-rabbit F4/80 antibody (1:50, 4 °C overnight) (ab100790, AbCam, Cambridge, UK).

Lipid Extraction and 2D High-Performance Thin-Layer Chromatography Analysis. Total lipids were extracted from lung homogenates by the Folch procedure.[57] Lipid extracts were separated and analyzed by 2D-HPTLC.[58] To prevent oxidative modification of phospholipids during separation, plates were treated with methanol containing 1 mM EDTA and 100 μM DTPA prior to application and separation of phospholipids by 2D-HPTLC. The phospholipids were visualized by exposure to iodine vapors and identified by comparison with authentic phospholipid standards. For electrospray ionization mass spectrometry (ESI-MS) and analysis of phospholipid hydroperoxides (PL-OOH) by fluorescence high-performance liquid chromatography (HPLC) using Amplex Red, the phospholipid spots on the silica plates were visualized by spraying the plates with deionized water. Subsequently, the spots were scraped from the silica plates and phospholipids were extracted in choloroform/methanol/water (10:5:1 v/v). Lipid phosphorus was determined by a micromethod.[59]

Oxidation of Total Lung Phospholipids by Cyt *c*/H_2O_2. Lipids extracted from lung of naive mice were dried under N_2 and resuspended in 50 mM Na and Na-phosphate buffer pH 7.4, containing 100 μM DTPA. Lipids (500 μM) were sonicated on ice/water for 20 min using high-performance ultrasonic system FS3 (Fisher Scientific, PA). Lipids were incubated with cyt *c* (10 μM) in the presence of H_2O_2 (100 μM) for 30 min at 37 °C. At the end of incubation lipids were extracted using the Folch procedure[57] and analyzed by LC/ESI-MS as described below.

Quantitation of Lipid Hydroperoxides. Lipid hydroperoxides were determined by fluorescence HPLC of resorufin formed in peroxidase-catalyzed reduction of specific PL-OOH with Amplex Red after hydrolysis by porcine pancreatic PLA_2 (1 U/μL) in 25 mM phosphate buffer containing 1.0 mM Ca, 0.5 mM EGTA, and 0.5 mM SDS (pH 8.0 at RT for 30 min). For the peroxidase reaction, 50 μM Amplex Red and microperoxidase-11 (1.0 μg/μL) were added to the hydrolyzed lipids, and the samples were incubated at 4 °C for 40 min. The reaction was started by addition of microperoxidase-11 and terminated by a stop reagent (100 μL of a solution of 10 mM HCl and 4 mM butylated hydroxytoluene in ethanol). The samples were centrifuged at 10000*g* for 5 min, and the supernatant was used for HPLC analysis. Aliquots (5 μL) were injected into a C_{18} reverse-phase column (Eclipse XDB-C18, 5 μm, 150 × 4.6 mm) and eluted using a mobile phase composed of 25 mM KH_2PO_4 (pH 7.0)/methanol (60:40 v/v) at a flow rate of 1 mL/min. The resorufin fluorescence was measured at 590 nm after excitation at 560 nm. A Shimadzu LC-100AT *vp* HPLC system equipped with a fluorescence detector (model RF-10Axl) and an autosampler (model SIL-10AD *vp*) was used.[23]

Electrospray Ionization Mass Spectrometry. LC/ESI-MS was performed using a Dionex Ultimate 3000 HPLC coupled online to ESI and a linear ion trap mass spectrometer (LXQ ThermoFisher). The lipids were separated on a normal-phase column (Luna 3 μm silica 100A, 150 × 2 mm (Phenomenex, Torrance CA)) with flow rate of 0.2 mL/min using gradient solvents containing 5 mM CH_3COONH_4 (A: *n*-hexane/2-propanol/water, 43:57:1 (v/v/v); B: *n*-hexane/2-propanol/water, 43:57:10 (v/v/v)). Analysis of phospholipid oxidized molecular species (hydroperoxy- and hydroxy-) was performed as described.[22,23] To minimize isotopic interferences between isolated masses M + 2, the spectra were acquired using an isolation width of 1.0 *m/z*. For identification of phopsholipids ESI-MS analysis was performed by direct infusion into an LXQ linear ion-trap mass spectrometer with the Xcalibur operating system (Thermo Fisher Scientific, San Jose, CA) as previously described.[23]

2D Liquid Chromatography Mass Spectrometry. CL separated by HPTLC was analyzed by LC/MS using a Prominence HPLC system (Shimadzu, Inc.) with a reverse-phase C_8 column (Luna, 5 μm, 4.6 mm × 15 cm, Phenomenex, Inc.). An isocratic solvent system (2-propanol/water/triethylamine/acetic acid (450:50:2.5:2.5, v/v/v/v)) was used at a flow rate of 0.4 mL/min. Spectra were analyzed on a Q-TOF Premier mass spectrometer (Waters, Inc.).

Parameters were as follows: capillary voltage, 2.85 kV, negative mode; source temperature, 100 °C; desolvation gas, 400 L/h; sampling cone, 60 V; extraction cone, 4.5 V; ion guide, 3.0 V. Tuning was optimized for oxidized and nonoxidized CL species across the CL scan range.

MALDI-TOF Mass Spectrometry. CL extracts were analyzed in triplicate on a Voyager DE-STR MALDI-TOF-MS (Applied Biosystems/Life Technologies, Carlsbad, CA). High-resolution mass measurements were done on an Ultraflex II MALDI-TOF-MS (Bruker Daltonics, Billerica, MA). Sample preparation was slightly modified from the method of Schiller *et al.*[60,61] In brief, the CL extract was spotted onto the MALDI target, followed by 500 mM 2,5-dihydroxybenzoic acid in methanol containing 0.02% trifluoroacetic acid. Spectra were acquired in reflector-negative mode with external calibration. Masses of all detected molecular species were confirmed to within 0.02 Da.

Liquid Chromatography/Electrospray Ionization Mass Spectrometry of Oxygenated Fatty Acids. Oxygenated fatty acids were analyzed by LC/ESI-MS after hydrolysis of major classes of phospholipids with porcine pancreatic PLA_2 (1 U/μL) in 25 mM phosphate buffer containing 1.0 mM Ca, 0.5 mM EGTA, and 0.5 mM SDS (pH 8.0 at RT for 30 min). Aliquots of extracted lipids (5 μL) were injected into a C_{18} reverse-phase column (Luna, 3 μm, 150 × 2 mm) and eluted using gradient solvents (A and B) containing 5 mM ammonium acetate at a flow rate of 0.2 mL/min. Solvent A was tetrahydrofuran/methanol/water/CH_3COOH, 25:30:50:0.1 (v/v/v/v). Solvent B was methanol/water, 90:10 (v/v). The column was eluted during the first 3 min isocratically at 50% B, from 3 to 23 min with a linear gradient from 50% solvent B to 98% solvent B, then 23−40 min isocratically using 98% solvent B, 40−42 min with a linear gradient from 98% solvent B to 50% solvent B, and 42−28 min isocratically using 50% solvent B for equilibration of the column. Hydroperoxy-fatty acids: 13*S*-OOH-9*Z*,11*E*-octadecadienoic acid, 9-OH-10*E*,12*Z*-octadeacadienoic acid, and 15*S*-OOH-5*Z*,8*Z*,11*Z*,13*E*-eicosatetraenoic acid from Cayman Chemicals (Ann Arbor, MI) were used as standards.

Statistics. The results are presented as mean ± SD values from at least three experiments, and statistical analyses were performed by either paired/unpaired Student's *t*-test or one-way ANOVA. The statistical significance of differences was set at $p < 0.05$.

Disclosure: The findings and conclusions in this report are those of the authors and do not necessarily represent the views of the National Institute for Occupational Safety and Health

Acknowledgment. This work was supported by NIOSH OH008282; by NIH HL70755, HL094488, U19AIO68021, and FP7-NANOMMUNE; and by NSF CHE-9808188 (Center for Molecular Analysis, Carnegie Mellon University). B.F. is supported by the Swedish Research Council (Senior Investigator Award for Inflammation Research).

Supporting Information Available: Accumulation of phospholipid hydroperoxides in the lung of mice exposed to SWCNTs (Table S1), assessment of CL molecular species in mouse lungs by LC/ESI-MS (Figure S1), LC/ESI-MS analysis of PS and PI from mice exposed to SWCNT (Figure S2), assessment of CL molecular species in mouse lung by MALDI-TOF-MS (Figure S3), identification of oxygenated fatty acids in CL obtained from the lung of mice exposed to SWCNTs (Figure S4), typical MS/MS spectra of oxygenated $C_{18:2}$ with *m/z* 311 after hydrolysis of PS and PI by PLA_2 (Figure S5). This material is available free of charge *via* the Internet at http://pubs.acs.org.

REFERENCES AND NOTES

1. Upadhyayula, V. K.; Deng, S.; Mitchell, M. C.; Smith, G. B. Application of Carbon Nanotube Technology for Removal of Contaminants in Drinking Water: A Review. *Sci. Total Environ.* **2009**, *408*, 1–13.
2. Malarkey, E. B.; Parpura, V. Applications of Carbon Nanotubes in Neurobiology. *Neurodegener. Dis.* **2007**, *4*, 292–299.
3. Klumpp, C.; Kostarelos, K.; Prato, M.; Bianco, A. Functionalized Carbon Nanotubes as Emerging Nanovectors for the Delivery of Therapeutics. *Biochim. Biophys. Acta* **2006**, *1758*, 404–412.
4. Firme, C. P., 3rd; Bandaru, P. R. Toxicity Issues in the Application of Carbon Nanotubes to Biological Systems. *Nanomedicine* **2010**, *6*, 245–256.
5. Chou, C. C.; Hsiao, H. Y.; Hong, Q. S.; Chen, C. H.; Peng, Y. W.; Chen, H. W.; Yang, P. C. Single-Walled Carbon Nanotubes Can Induce Pulmonary Injury in Mouse Model. *Nano Lett.* **2008**, *8*, 437–445.
6. Shvedova, A. A.; Kisin, E. R.; Mercer, R.; Murray, A. R.; Johnson, V. J.; Potapovich, A. I.; Tyurina, Y. Y.; Gorelik, O.; Arepalli, S.; Schwegler-Berry, D.; *et al*. Unusual Inflammatory and Fibrogenic Pulmonary Responses to Single-Walled Carbon Nanotubes in Mice. *Am. J. Physiol. Lung Cell Mol. Physiol.* **2005**, *289*, L698–708.
7. Shvedova, A. A.; Kisin, E. R.; Murray, A. R.; Kommineni, C.; Castranova, V.; Fadeel, B.; Kagan, V. E. Increased Accumulation of Neutrophils and Decreased Fibrosis in the Lung of NADPH Oxidase-Deficient C57BL/6 Mice Exposed to Carbon Nanotubes. *Toxicol. Appl. Pharmacol.* **2008**, *231*, 235–240.
8. Song, Y.; Li, X.; Du, X. Exposure to Nanoparticles is Related to Pleural Effusion, Pulmonary Fibrosis and Granuloma. *Eur. Respir. J.* **2009**, *34*, 559–567.
9. Wu, M.; Gordon, R. E.; Herbert, R.; Padilla, M.; Moline, J.; Mendelson, D.; Litle, V.; Travis, W. D.; Gil, J. Case Report: Lung Disease in World Trade Center Responders Exposed to Dust and Smoke: Carbon Nanotubes Found in the Lungs of World Trade Center Patients and Dust Samples. *Environ. Health Perspect.* **2010**, *118*, 499–504.
10. Nel, A.; Xia, T.; Madler, L.; Li, N. Toxic Potential of Materials at the Nanolevel. *Science* **2006**, *311*, 622–627.
11. Jacobsen, N. R.; Pojana, G.; White, P.; Moller, P.; Cohn, C. A.; Korsholm, K. S.; Vogel, U.; Marcomini, A.; Loft, S.; Wallin, H. Genotoxicity, Cytotoxicity, and Reactive Oxygen Species Induced by Single-Walled Carbon Nanotubes and C(60) Fullerenes in the FE1-Mutatrade Mark Mouse Lung Epithelial Cells. *Environ. Mol. Mutagen.* **2008**, *49*, 476–487.
12. Kagan, V. E.; Tyurina, Y. Y.; Tyurin, V. A.; Konduru, N. V.; Potapovich, A. I.; Osipov, A. N.; Kisin, E. R.; Schwegler-Berry, D.; Mercer, R.; Castranova, V.; *et al*. Direct and Indirect Effects of Single Walled Carbon Nanotubes on RAW 264.7 Macrophages: Role of Iron. *Toxicol. Lett.* **2006**, *165*, 88–100.
13. Sharma, C. S.; Sarkar, S.; Periyakaruppan, A.; Barr, J.; Wise, K.; Thomas, R.; Wilson, B. L.; Ramesh, G. T. Single-Walled Carbon Nanotubes Induces Oxidative Stress in Rat Lung Epithelial Cells. *J. Nanosci. Nanotechnol.* **2007**, *7*, 2466–2472.
14. Shvedova, A. A.; Kisin, E. R.; Murray, A. R.; Gorelik, O.; Arepalli, S.; Castranova, V.; Young, S. H.; Gao, F.; Tyurina, Y. Y.; Oury, T. D.; *et al*. Vitamin E Deficiency Enhances Pulmonary Inflammatory Response and Oxidative Stress Induced by Single-Walled Carbon Nanotubes in C57BL/6 Mice. *Toxicol. Appl. Pharmacol.* **2007**, *221*, 339–348.
15. Aoki, H.; Hisada, T.; Ishizuka, T.; Utsugi, M.; Kawata, T.; Shimizu, Y.; Okajima, F.; Dobashi, K.; Mori, M. Resolvin E1 Dampens Airway Inflammation and Hyperresponsiveness in a Murine Model of Asthma. *Biochem. Biophys. Res. Commun.* **2008**, *367*, 509–515.
16. Haworth, O.; Cernadas, M.; Yang, R.; Serhan, C. N.; Levy, B. D. Resolvin E1 Regulates Interleukin 23, Interferon-Gamma and Lipoxin A4 to Promote the Resolution of Allergic Airway Inflammation. *Nat. Immunol.* **2008**, *9*, 873–879.
17. Clark, S. R.; Guy, C. J.; Scurr, M. J.; Taylor, P. R.; Kift-Morgan, A. P.; Hammond, V. J.; Thomas, C. P.; Coles, B.; Roberts, G. W.; Eberl, M.; *et al*. Esterified Eicosanoids Are Acutely Generated by 5-Lipoxygenase in Primary Human Neutrophils and in Human and Murine Infection. *Blood* **2011**, *117*, 2033–2043.
18. Fadeel, B.; Xue, D. The Ins and Outs of Phospholipid Asymmetry in the Plasma Membrane: Roles in Health and Disease. *Crit. Rev. Biochem. Mol. Biol.* **2009**, *44*, 264–277.
19. Tyurina, Y. Y.; Tyurin, V. A.; Zhao, Q.; Djukic, M.; Quinn, P. J.; Pitt, B. R.; Kagan, V. E. Oxidation of Phosphatidylserine: a Mechanism for Plasma Membrane Phospholipid Scrambling during Apoptosis?. *Biochem. Biophys. Res. Commun.* **2004**, *324*, 1059–1064.

20. Kagan, V. E.; Borisenko, G. G.; Serinkan, B. F.; Tyurina, Y. Y.; Tyurin, V. A.; Jiang, J.; Liu, S. X.; Shvedova, A. A.; Fabisiak, J. P.; Uthaisang, W.; *et al*. Appetizing Rancidity of Apoptotic Cells for Macrophages: Oxidation, Externalization, and Recognition of Phosphatidylserine. *Am. J. Physiol. Lung Cell Mol. Physiol.* **2003**, *285*, L1–17.
21. Kagan, V. E.; Konduru, N. V.; Feng, W.; Allen, B. L.; Conroy, J.; Volkov, Y.; Vlasova, I. I.; Belikova, N. A.; Yanamala, N.; Kapralov, A.; *et al*. Carbon Nanotubes Degraded by Neutrophil Myeloperoxidase Induce Less Pulmonary Inflammation. *Nat. Nanotechnol.* **2010**, *5*, 354–359.
22. Shvedova, A. A.; Kagan, V. E.; Fadeel, B. Close Encounters of the Small Kind: Adverse Effects of Man-Made Materials Interfacing with the Nano-Cosmos of Biological Systems. *Annu. Rev. Pharmacol. Toxicol.* **2010**, *50*, 63–88.
23. Tyurin, V. A.; Tyurina, Y. Y.; Ritov, V. B.; Lysytsya, A.; Amoscato, A. A.; Kochanek, P. M.; Hamilton, R.; Dekosky, S. T.; Greenberger, J. S.; Bayir, H.; *et al*. Oxidative Lipidomics of Apoptosis: Quantitative Assessment of Phospholipid Hydroperoxides in Cells and Tissues. *Methods Mol. Biol.* **2010**, *610*, 353–374.
24. Tyurina, Y. Y.; Tyurin, V. A.; Kapralova, V. I.; Wasserloos, K.; Mosher, M.; Epperly, M. W.; Greenberger, J. S.; Pitt, B. R.; Kagan, V. E. Oxidative Lipidomics of Gamma-Radiation-Induced Lung Injury: Mass Spectrometric Characterization of Cardiolipin and Phosphatidylserine Peroxidation. *Radiat. Res.* **2011**, *175*, 610–621.
25. Tyurina, Y. Y.; Tyurin, V. A.; Kapralova, V. I.; Amoscato, A. A.; Epperly, M. W.; Greenberger, J. S.; Kagan, V. E. Mass-Spectrometric Characterization of Phospholipids and Their Hydroperoxide Derivatives *in Vivo*: Rffects of Total Body Irradiation. *Methods Mol. Biol.* **2009**, *580*, 153–183.
26. Shvedova, A. A.; Kisin, E.; Murray, A. R.; Johnson, V. J.; Gorelik, O.; Arepalli, S.; Hubbs, A. F.; Mercer, R. R.; Keohavong, P.; Sussman, N.; *et al*. Inhalation *vs.* Aspiration of Single-Walled Carbon Nanotubes in C57BL/6 Mice: Inflammation, Fibrosis, Oxidative Stress, and Mutagenesis. *Am. J. Physiol. Lung Cell Mol. Physiol.* **2008**, *295*, L552–565.
27. Kagan, V. E. *Lipid Peroxidation in Biomembranes*; CRC Press: Boca Raton, FL, 1988.
28. Kapralov, A. A.; Kurnikov, I. V.; Vlasova, I. I.; Belikova, N. A.; Tyurin, V. A.; Basova, L. V.; Zhao, Q.; Tyurina, Y. Y.; Jiang, J.; Bayir, H.; *et al*. The Hierarchy of Structural Transitions Induced in Cytochrome c by Anionic Phospholipids Determines Its Peroxidase Activation and Selective Peroxidation during Apoptosis in Cells. *Biochemistry* **2007**, *46*, 14232–14244.
29. Bayir, H.; Tyurin, V. A.; Tyurina, Y. Y.; Viner, R.; Ritov, V.; Amoscato, A. A.; Zhao, Q.; Zhang, X. J.; Janesko-Feldman, K. L.; Alexander, H.; *et al*. Selective Early Cardiolipin Peroxidation after Traumatic Brain Injury: an Oxidative Lipidomics Analysis. *Ann. Neurol.* **2007**, *62*, 154–169.
30. Tyurin, V. A.; Tyurina, Y. Y.; Jung, M. Y.; Tungekar, M. A.; Wasserloos, K. J.; Bayir, H.; Greenberger, J. S.; Kochanek, P. M.; Shvedova, A. A.; Pitt, B.; *et al*. Mass-Spectrometric Analysis of Hydroperoxy- and Hydroxy-Derivatives of Cardiolipin and Phosphatidylserine in Cells and Tissues Induced by Pro-apoptotic and Pro-inflammatory Stimuli. *J. Chromatogr. B: Analyt. Technol. Biomed. Life Sci.* **2009**, *877*, 2863–2872.
31. Kagan, V. E.; Bayir, H. A.; Belikova, N. A.; Kapralov, O.; Tyurina, Y. Y.; Tyurin, V. A.; Jiang, J.; Stoyanovsky, D. A.; Wipf, P.; Kochanek, P. M.; *et al*. Cytochrome c/Cardiolipin Relations in Mitochondria: A Kiss of Death. *Free Radical Biol. Med.* **2009**, *46*, 1439–1453.
32. Tyurin, V. A.; Tyurina, Y. Y.; Feng, W.; Mnuskin, A.; Jiang, J.; Tang, M.; Zhang, X.; Zhao, Q.; Kochanek, P. M.; Clark, R. S.; *et al*. Mass-Spectrometric Characterization of Phospholipids and Their Primary Peroxidation Products in Rat Cortical Neurons during Staurosporine-Induced Apoptosis. *J. Neurochem.* **2008**, *107*, 1614–1633.
33. Tyurina, Y. Y.; Tyurin, V. A.; Epperly, M. W.; Greenberger, J. S.; Kagan, V. E. Oxidative Lipidomics of Gamma-Irradiation-Induced Intestinal Injury. *Free Radical Biol. Med.* **2008**, *44*, 299–314.
34. Maynard, A. D.; Baron, P. A.; Foley, M.; Shvedova, A. A.; Kisin, E. R.; Castranova, V. Exposure to Carbon Nanotube Material: Aerosol Release during the Handling of Unrefined Single-Walled Carbon Nanotube Material. *J. Toxicol. Environ. Health A* **2004**, *67*, 87–107.
35. EPA, 40 CFR Part 50. National Ambient Air Quality Standards or Particulate Matter. Final Rule volume 71, No. 200, **2006**.
36. Deng, X.; Jia, G.; Wang, H.; Sun, H.; Wang, X.; Yang, S.; Wang, T.; Liu, Y. Translocation and Fate of Multi-Walled Carbon Nanotubes *in Vivo*. *Carbon* **2007**, *45*, 1419–1424.
37. Folkmann, J. K.; Risom, L.; Jacobsen, N. R.; Wallin, H.; Loft, S.; Moller, P. Oxidatively Damaged DNA in Rats Exposed by Oral Gavage to C60 Fullerenes and Single-Walled Carbon Nanotubes. *Environ. Health Perspect.* **2009**, *117*, 703–708.
38. Danial, N. N.; Korsmeyer, S. J. Cell Death: Critical Control Points. *Cell* **2004**, *116*, 205–219.
39. Kagan, V. E.; Tyurin, V. A.; Jiang, J.; Tyurina, Y. Y.; Ritov, V. B.; Amoscato, A. A.; Osipov, A. N.; Belikova, N. A.; Kapralov, A. A.; Kini, V.; *et al*. Cytochrome c Acts as a Cardiolipin Oxygenase Required for Release of Proapoptotic Factors. *Nat. Chem. Biol.* **2005**, *1*, 223–232.
40. Belikova, N. A.; Vladimirov, Y. A.; Osipov, A. N.; Kapralov, A. A.; Tyurin, V. A.; Potapovich, M. V.; Basova, L. V.; Peterson, J.; Kurnikov, I. V.; Kagan, V. E. Peroxidase Activity and Structural Transitions of Cytochrome c Bound to Cardiolipin-Containing Membranes. *Biochemistry* **2006**, *45*, 4998–5009.
41. Wipf, P.; Xiao, J.; Jiang, J.; Belikova, N. A.; Tyurin, V. A.; Fink, M. P.; Kagan, V. E. Mitochondrial Targeting of Selective Electron Scavengers: Synthesis and Biological Analysis of Hemigramicidin-TEMPO Conjugates. *J. Am. Chem. Soc.* **2005**, *127*, 12460–12461.
42. Kagan, V. E.; Wipf, P.; Stoyanovsky, D.; Greenberger, J. S.; Borisenko, G.; Belikova, N. A.; Yanamala, N.; Samhan Arias, A. K.; Tungekar, M. A.; Jiang, J.; *et al*. Mitochondrial Targeting of Electron Scavenging Antioxidants: Regulation of Selective Oxidation *vs* Random Chain Reactions. *Adv. Drug Delivery Rev.* **2009**, *61*, 1375–1385.
43. Tyurina, Y. Y.; Tyurin, V. A.; Kaynar, A. M.; Kapralova, V. I.; Wasserloos, K.; Li, J.; Mosher, M.; Wright, L.; Wipf, P.; Watkins, S.; *et al*. Oxidative Lipidomics of Hyperoxic Acute Lung Injury: Mass Spectrometric Characterization of Cardiolipin and Phosphatidylserine Peroxidation. *Am. J. Physiol. Lung Cell Mol. Physiol.* **2010**, *299*, L73–85.
44. Jiang, J.; Belikova, N. A.; Hoye, A. T.; Zhao, Q.; Epperly, M. W.; Greenberger, J. S.; Wipf, P.; Kagan, V. E. A Mitochondria-Targeted Nitroxide/Hemigramicidin S Conjugate Protects Mouse Embryonic Cells against Gamma Irradiation. *Int. J. Radiat. Oncol. Biol. Phys.* **2008**, *70*, 816–825.
45. Rwigema, J. C.; Beck, B.; Wang, W.; Doemling, A.; Epperly, M. W.; Shields, D.; Goff, J. P.; Franicola, D.; Dixon, T.; Frantz, M. C.; *et al*. Two Strategies for the Development of Mitochondrion-Targeted Small Molecule Radiation Damage Mitigators. *Int. J. Radiat. Oncol. Biol. Phys.* **2011**, *80*, 860–868.
46. Fadeel, B.; Xue, D.; Kagan, V. Programmed Cell Clearance: Molecular Regulation of the Elimination of Apoptotic Cell Corpses and Its Role in the Resolution of Inflammation. *Biochem. Biophys. Res. Commun.* **2010**, *396*, 7–10.
47. Kagan, V. E.; Borisenko, G. G.; Tyurina, Y. Y.; Tyurin, V. A.; Jiang, J.; Potapovich, A. I.; Kini, V.; Amoscato, A. A.; Fujii, Y. Oxidative Lipidomics of Apoptosis: Redox Catalytic Interactions of Cytochrome c with Cardiolipin and Phosphatidylserine. *Free Radical Biol. Med.* **2004**, *37*, 1963–1985.
48. Tyurina, Y. Y.; Kawai, K.; Tyurin, V. A.; Liu, S. X.; Kagan, V. E.; Fabisiak, J. P. The Plasma Membrane is the Site of Selective Phosphatidylserine Oxidation during Apoptosis: Role of Cytochrome c. *Antioxid. Redox Signal* **2004**, *6*, 209–225.
49. Fadeel, B. Plasma Membrane Alterations during Apoptosis: Role in Corpse Clearance. *Antioxid. Redox Signal* **2004**, *6*, 269–275.
50. Arroyo, A.; Modriansky, M.; Serinkan, F. B.; Bello, R. I.; Matsura, T.; Jiang, J.; Tyurin, V. A.; Tyurina, Y. Y.; Fadeel, B.; Kagan, V. E. NADPH Oxidase-Dependent Oxidation and

Externalization of Phosphatidylserine during Apoptosis in Me_2SO-Differentiated HL-60 Cells. Role in Phagocytic Clearance. *J. Biol. Chem.* **2002**, *277*, 49965–49975.
51. Kagan, V. E.; Gleiss, B.; Tyurina, Y. Y.; Tyurin, V. A.; Elenstrom-Magnusson, C.; Liu, S. X.; Serinkan, F. B.; Arroyo, A.; Chandra, J.; Orrenius, S.; *et al*. A Role for Oxidative Stress in Apoptosis: Oxidation and Externalization of Phosphatidylserine Is Required for Macrophage Clearance of Cells Undergoing Fas-Mediated Apoptosis. *J. Immunol.* **2002**, *169*, 487–499.
52. Greenberg, M. E.; Sun, M.; Zhang, R.; Febbraio, M.; Silverstein, R.; Hazen, S. L. Oxidized Phosphatidylserine-CD36 Interactions Play an Essential Role in Macrophage-Dependent Phagocytosis of Apoptotic Cells. *J. Exp. Med.* **2006**, *203*, 2613–2625.
53. Sanmun, D.; Witasp, E.; Jitkaew, S.; Tyurina, Y. Y.; Kagan, V. E.; Ahlin, A.; Palmblad, J.; Fadeel, B. Involvement of a Functional NADPH Oxidase in Neutrophils and Macrophages during Programmed Cell Clearance: Implications for Chronic Granulomatous Disease. *Am. J. Physiol. Cell Physiol.* **2009**, *297*, C621–631.
54. Green, J. T.; Orr, S. K.; Bazinet, R. P. The Emerging Role of Group VI Calcium-Independent Phospholipase A2 in Releasing Docosahexaenoic Acid from Brain Phospholipids. *J. Lipid Res.* **2008**, *49*, 939–944.
55. Moller, P.; Jacobsen, N. R.; Folkmann, J. K.; Danielsen, P. H.; Mikkelsen, L.; Hemmingsen, J. G.; Vesterdal, L. K.; Forchhammer, L.; Wallin, H.; Loft, S. Role of Oxidative Damage in Toxicity of Particulates. *Free Radical Res.* **2010**, *44*, 1–46.
56. Reddy, A. R.; Rao, M. V.; Krishna, D. R.; Himabindu, V.; Reddy, Y. N. Evaluation of Oxidative Stress and Anti-Oxidant Status in Rat Serum Following Exposure of Carbon Nanotubes. *Regul. Toxicol. Pharmacol.* **2011**, *59*, 251–257.
57. Folch, J.; Lees, M.; Sloane Stanley, G. H. A Simple Method for the Isolation and Purification of Total Lipides from Animal Tissues. *J. Biol. Chem.* **1957**, *226*, 497–509.
58. Rouser, G.; Fkeischer, S.; Yamamoto, A. Two Dimensional Thin Layer Chromatographic Separation of Polar Lipids and Determination of Phospholipids by Phosphorus Analysis of Spots. *Lipids* **1970**, *5*, 494–496.
59. Bottcher, C. J. F.; Van Gent, C. M.; Pries, C. A Rapid and Sensitive Sub-Micro Phosphorus Determination. *Anal. Chim. Acta* **1961**, *24*, 203–204.
60. Schiller, J.; Suss, R.; Arnhold, J.; Fuchs, B.; Lessig, J.; Muller, M.; Petkovic, M.; Spalteholz, H.; Zschornig, O.; Arnold, K. Matrix-Assisted Laser Desorption and Ionization Time-of-Flight (MALDI-TOF) Mass Spectrometry in Lipid and Phospholipid Research. *Prog. Lipid Res.* **2004**, *43*, 449–488.
61. Schiller, J.; Suss, R.; Fuchs, B.; Muller, M.; Zschornig, O.; Arnold, K. MALDI-TOF MS in Lipidomics. *Front. Biosci.* **2007**, *12*, 2568–2579.